Natural Resources Canada | Ressources naturelles Canada

Trace element characteristics and S isotopic compositions of pyrite in the Howard's Pass Zn-Pb District, Selwyn Basin, Yukon

M. Gadd[1†], D. Layton-Matthews[1], J. Peter[2] and S. Paradis[3]
[1]Queen's University, Kingston, Ontario; [2]Geological Survey of Canada, Ottawa, Ontario;
[3]Geological Survey of Canada, Sidney, British Columbia
† Contact information: michael.gadd@queensu.ca

Rationale and Purpose

The Howard's Pass Zn-Pb district (HPD) is a sedimentary exhalative (SEDEX) district comprising 14 Zn-Pb deposits that contain an estimated 400Mt of Zn and Pb grading at 5% and 2%, respectively (Goodfellow, 1993). The HPD is located within the Selwyn Basin, a prolific metallogenic province that is primarily known for its world-class Zn-Pb (±Ag ±Ba) SEDEX deposits (Fig. 1). Pyrite is a minor but ubiquitous component of the sulfide mineralogy, which is dominantly comprised of sphalerite and galena, and is also present in the host carbonaceous mudstones in the HPD. We have used electron probe microanalysis-wavelength dispersive spectrometry (EPMA-WDS), laser ablation-inductively couple plasma mass spectrometry (LA-ICP-MS) and secondary ion mass spectrometry (SIMS) to determine the major element chemistry, trace element chemistry and S isotopic compositions, respectively, of the different textural varieties of pyrite throughout the stratigraphic succession that hosts SEDEX mineralization at the HPD.

Petrographic, LA-ICPMS and EPMA-WDS data provide information on the composition and relative timing of depositional, diagenetic and metamorphic fluids responsible for multiple generations of pyrite formation. SIMS data reveal trends in the sulphur isotopic compositions of pyrites and offer new insight into the redox conditions of the ambient marine bottom waters in which framboidal pyrites were precipitated. These data suggest that the timing of hydrothermal SEDEX fluids were not coeval with sedimentation, but are synchronous with diagenesis.

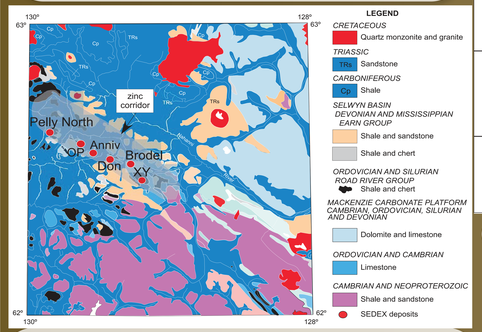


Fig. 1: Geological map showing significant SEDEX deposits in the 'Zinc Corridor' (the broad area within which Zn mineralization occurs; modified from Goodfellow, 2004).

District Geology

The HPD is located in the Selwyn Basin, Yukon, an Upper Proterozoic to Paleozoic continental margin basin filled by thick successions of fine-grained siliciclastic and calcareous sedimentary rocks (Goodfellow, 2004). SEDEX mineralization in the HPD is hosted in a succession of Llandoverian carbonaceous calcareous to siliceous mudstones and limestones (Fig. 2; Gordey and Anderson, 1993). The Llandoverian strata that contain SEDEX mineralization are collectively referred to as the Active Member (ACTM; Morganti, 1979).

Zn-Pb mineralization within the ACTM is predominantly comprised of sphalerite and galena. Sphalerite occurs as fine laminae (<1mm), interlaminated with galena and framboidal pyrite. Non-laminated sphalerite occurs less commonly as light brown crystalline blebs. Galena occurs within laminae associated with sphalerite; however, high-grade galena mineralization occurs predominantly as cleavage controlled stringers. The ACTM has three mineralized sub-units: 1) finely laminated dark grey to brown mudstone, 2) calcareous white to grey Zn-Pb-rich mudstone and 3) silicic white to grey Zn-Pb-rich mudstone. The SEDEX mineralization has been interpreted to be the product of venting of hydrothermal fluids and precipitation of fine-grained sulphide minerals near the seafloor, where the laminae were rhythmically deposited (Goodfellow, 1984, 2004).

Younger SEDEX(?) deposits in the HPD are present in the Middle Silurian Upper Siliceous Mudstone (USMS) and Lower Devonian Backside Siliceous Mudstone (BSSM). These deposits occur as thin (<0.5m) and discontinuous lenses and contain disseminated sphalerite and framboidal pyrite.

Acknowledgements

This project is jointly funded by NSERC, CAMIRO and the TGI-4 program of the Geological Survey of Canada. We sincerely thank SEGCF for financial support and Jason Dunning, Gabe Xue, Wolfgang Schleiss and Jelle de Bruyckere of Selwyn Chihong Mining Ltd. for providing transportation, lodging, access to core, samples and technical information. We also greatly appreciate time spent in the field with Duncan Bain and Bob Hodder and for their insightful discussions with us on many aspects of Selwyn Basin geology and SEDEX deposit genesis.

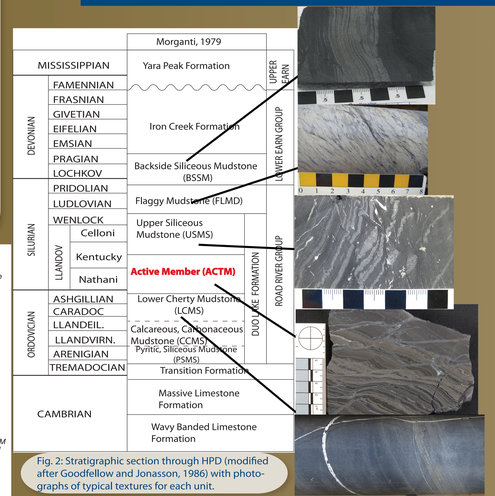
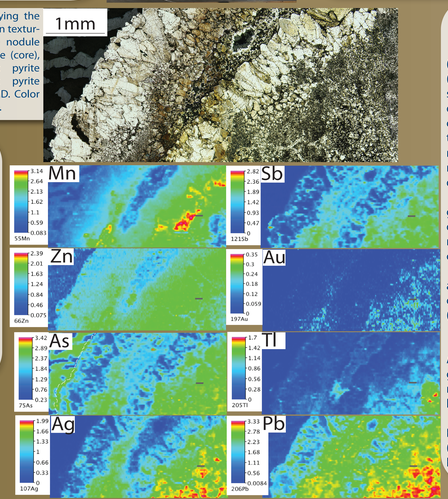


Fig. 2: Stratigraphic section through HPD (modified after Goodfellow and Jonasson, 1986) with photographs of typical textures for each unit.

Fig. 4: LA-ICP-MS map displaying the distribution of trace elements in texturally zoned diagenetic pyrite nodule consisting of framboidal pyrite (core), sooty to clear diagenetic pyrite (mantle) and metamorphic pyrite (outermost rim) from the FLMD. Color ramps are nonlinear $\log_{10}$ ppm.



Pyrite Morphology and Paragenesis

Pyrite framboids and minute euhedra (py1) consist of fine-grained laminated concentrations and disseminated clusters of pyrite parallel to bedding (Fig. 3A). The highest accumulations py1 occur in the Zn-Pb mineralization of the ACTM where it forms delicately laminated, mm-scale beds intercalated with carbonaceous sediments, sphalerite and galena. In general, however, py1 is subordinate to the other textural type of pyrite.

Bedding-parallel pyrite bands (py2a) occur as wispy laminae to aggregated and intergrown subhedral to euhedral crystals (Fig. 3B). Py2a forms as wispy and discontinuous bands to well-formed and continuous beds at the drill core scale. Wispy py2a differs from laminated py1 in that the framboidal texture is either overprinted or obliterated due to recrystallization.

Pyrite nodules (py2b) comprise spheroidal masses of intergrown and aggregated subhedral pyrite crystals that commonly show radial growth patterns and herringbone textures (Fig. 3C). Py2b nodules commonly display complex growth textures that range from sooty (silicate inclusion-rich) to clear (inclusion-free).

Metamorphic pyrite (py3) occurs as euhedral crystals and thin overgrowths. Py3 is the latest stage of pyrite growth in the HPD and overgrows all preceding generations of pyrite (Fig. 3D). Euhedral py3 crystals are between 0.1 mm and 50 mm and are crystallographically aligned with the regional cleavage. Metamorphic overgrowths are <0.2mm wide and form as veneers on diagenetic pyrites.

Sphalerite, galena and chalcopyrite occur together with pyrite in the Road River and Lower Earn groups. Sphalerite and galena inclusions in pyrite occur as fracture fillings within and interstitial to adjacent pyrite crystals, and they are most common in the rocks immediately above and below Zn-Pb mineralization. Chalcopyrite forms interstitially between adjacent pyrite crystals, and less commonly as discrete subhedral overgrowths on pyrite. Chalcopyrite is distributed throughout the HPD stratigraphic succession, but is present in conspicuously low abundances in the Zn-Pb mineralization.

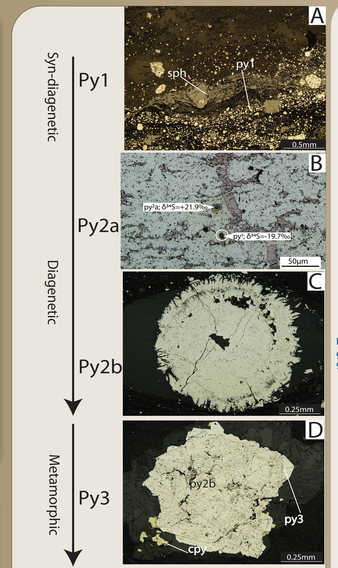


Fig. 3: The interpreted stages of pyrite formation in the HPD. Samples are from A) XYC-190-372.0 (ACTM), B) Don-200-387.0 (ACTM; Au-coated), C) Don-76-221.9 (CCMS) and D) XYC-224-133.3 (USMS).

Results: LA-ICP-MS

The trace element compositions of py1 (n=114), py2a (n=144), py2b (n=229) and py3 (n=112) were determined by LA-ICP-MS. A series of line rasters across pyrite crystals were employed to measure the distributions and contents of minor and trace elements. Pyrite in the HPD contains a broad suite of trace elements, the most abundant of which are Mn, Ni, Cu, Zn, As, Se, Ag, Sb, Au, Tl and Pb. The content of these elements varies between pyrite generations and stratigraphic position. Trace element variability in pyrites that display multiple growth zones is coincident with textural and morphological variability (Fig. 4).

Median Se, Ag, Sb, Au, Tl and Pb contents in pyrite display the most variability (1 order of magnitude or greater) between py1 and subsequent generations (Fig. 5). Median V, Mn, Ni, Cu, Zn and As contents in pyrite display less variability (<1 order of magnitude) between py1 and subsequent generations (Fig. 5). Trace element contents generally decrease as a function of relative age, where the highest contents are in py1 and decrease in py2a, b. Py3 typically has the lowest trace element contents.

Trace element contents of pyrite in the HPD stratigraphic succession are zoned. Median V, Mn, Ni, Se, Au, Tl and Pb contents in pyrite display the most variability (1 order of magnitude or greater) from the base to the top of the stratigraphic succession (Fig. 6). Median Cu, Zn, As, Ag, and Sb contents in pyrite display less variability (<1 order of magnitude) from the base to the top of the stratigraphic succession (Fig. 6).

Results: SIMS

Analytical spots (n=99) were selected using a combination of BSE images and EPMA-WDS maps. Each pyrite generation displays a broad range of $\delta^{34}S$ values (Fig. 7). Sulfur isotope ratios vary between pyrite generations, mimicking textural and trace element variability at the sub-millimeter scale. All SIMS S isotope data are calculated using Vienna Cañon Diablo troilite and are reported as permil (‰).

Framboidal py1 within SEDEX mineralization hosted by the Early Silurian ACTM, and within a thin (<0.5 m) Early Devonian framboidal pyrite-laminated sphalerite SEDEX(?) deposit record the most negative $\delta^{34}S$ values (-21.9 to -4.6). Py1 analyses from the FLMD and USMS yield positive $\delta^{34}S$ values (10.3 and 20.0, respectively), however these are not associated with SEDEX mineralization.

Recommended citation
Gadd, M., Layton-Matthews, D., Peter, J., and Paradis, S., 2014. Trace element characteristics and S isotopic compositions of pyrite in the Howard's Pass Zn-Pb District, Selwyn Basin, Yukon; Geological Survey of Canada, Open File 7511, 1 poster. doi:10.4095/293468

©Her Majesty the Queen in Right of Canada 2014
doi:10.4095/293468

This publication is available for free download through GEOSCAN (http://geoscan.ess.nrcan.gc.ca/).

OPEN FILE
DOSSIER PUBLIC
7511
GEOLOGICAL SURVEY OF CANADA
COMMISSION GÉOLOGIQUE DU CANADA
2014
Publications in this series have not been edited; they are released as submitted by the author.
Les publications de cette série ne sont pas révisées; elles sont publiées telles que soumises par l'auteur.

Canada

Targeted Geoscience Intiative 4: Increasing Deep Exploration Effectiveness

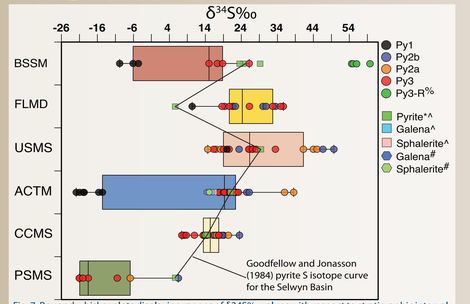


Fig. 7: Box and whisker plots displaying ranges of δ34S‰ values with respect to stratigraphic interval. Boxes outline the 25 to 75 percentiles and whiskers extend to extreme data points. Py3-R%: replacing barite, not included in the box and whisker statistics; *Goodfellow and Jonasson (1984), ^Goodfellow and Jonasson (1986), # Cleland (2008): not included in statistics.

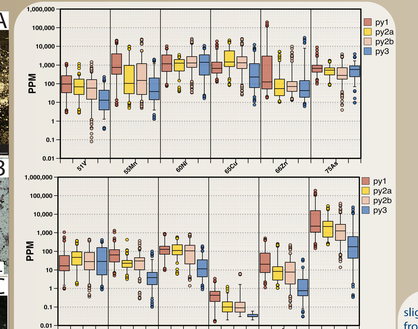


Fig. 5: Box and whisker plots of trace element content ranges with respect to pyrite generation. Boxes outline the 25th to 75th percentiles and whiskers extend to 5th and 95th percentiles.

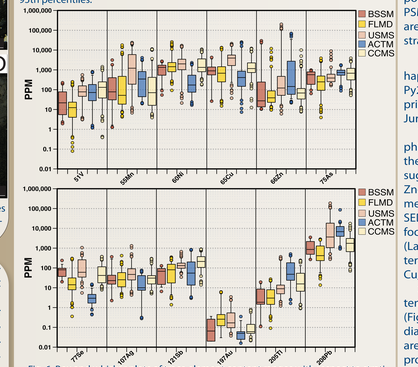


Fig. 6: Box and whisker plots of trace element content ranges with respect to stratigraphic interval. Boxes outline the 25th to 75th percentiles and whiskers extend to 5th and 95 percentiles.

Py2a and py2b from the PSMS (i.e., lowermost Duo Lake Formation) to the USMS record slightly negative to highly positive $\delta^{34}S$ values (-6.9 to 49.7) and systematically (?) increase from the base to the top of the Duo Lake Formation (Fig. 7). Diagenetic pyrite $\delta^{34}S$ in the FLMD are slightly lower than those in the USMS (22.3 to 33.5).

Metamorphic euhedral and overgrowth py3 $\delta^{34}S$ values range from moderately to highly positive (7.5 to 35.7) and trend similarly to py2a and py2b (CCMS to FLMD). Py3 from the PSMS has highly negative $\delta^{34}S$ values (-21.1 to -10.5); however, these metamorphic pyrites are petrographically consistent with py3 metamorphic overgrowths observed higher in the stratigraphy.

Discussion and Conclusions

Py1 in the HPD is interpreted to have formed as syngenetic chemical sediments, and perhaps into the earliest stages of diagenesis, from bacterially reduced ambient seawater sulfate. Py2a, b are interpreted to have formed during early to late diagenesis in carbonaceous muds prior to lithification. Py3 overgrowths and euhedra are interpreted to have formed during Late Jurassic to Early Cretaceous cleavage development and orogenesis.

Trace element contents are generally higher in diagenetic py1, 2a, b relative to metamorphic py3 (Figs. 4, 5). The contents of Mn, Zn, Ag, Tl, Pb and V in pyrite are high in the ACTM and the immediate host carbonaceous mudstones, and are lower in the FLMD and BSSM (Fig. 6), suggesting that these elements were sourced from the SEDEX mineralizing fluids. Thallium-Zn-Pb-bearing pyrite (py1, 2a, b) extends into the stratigraphic hanging wall and footwall sediments (Figs. 4, 6), and laterally along the Zn Corridor in the HPD. A Zn-Pb-Tl halo in the HYC SEDEX deposit is known to extend more than 100m into the stratigraphic hanging wall and footwall of the host carbonaceous sediments, and laterally along pyritic black shale facies (Large et al., 2000). Elements in pyrite that likely reflect redox conditions of diagenetic porewaters are not associated with SEDEX mineralization, but are of hydrogenous origin, include Ni, Cu, Se and Au.

Sulphur isotope ratios in diagenetic pyrites (py2a, b) display a trend that is generally consistent with diagenetic pyrite sulfur isotope ratios reported by Goodfellow and Jonasson (1984) (Fig. 7). However, preliminary SIMS py1 sulphur isotope ratios strongly contrast those of bulk diagenetic pyrites previously reported in SEDEX mineralization. The most striking variations are between py1 and later overgrowths in the ACTM. Framboidal pyrite adjacent to or in close proximity to diagenetic py2a, b display variability of up to 40 $\delta^{34}S$ (Figs. 3B, 7).

Jonasson and Goodfellow (1986) interpreted framboidal pyrite in the ACTM to have coprecipitated with sphalerite and galena in a persistently euxinic water column within a restricted basin. Framboidal pyrite precipitation in low temperature sedimentary environments records ambient sulphur isotopic compositions (Lyons, 1997). If a $\delta^{34}S$ fractionation factor of 40 is assumed between bacterially reduced sulphate and resultant sulphide (Sweeney and Kaplan, 1980), then $\delta^{34}S$ values for framboidal pyrite in the HPD SEDEX deposits are consistent with derivation of sulphide from coeval seawater sulphate (Claypool et al., 1980). Sphalerite and galena $\delta^{34}S$ values are much heavier than framboidal pyrite (Fig. 7), implying that that the coprecipitation of framboidal pyrite, sphalerite and galena did not occur.

Because diagenetic pyrite overgrowth textures clearly postdate framboid precipitation and sphalerite and galena do not record ambient sulphur isotope ratios (Fig. 7), it is improbable that framboidal pyrite shares a source of sulphur with the bulk of the base metal sulfides. These minerals were thought to have all precipitated from a common source of H_2S accumulated in the water column, and with similar $\delta^{34}S$ values for pyrite, sphalerite and galena (Goodfellow, 1987). The isotopically light pyrite likely formed differently from isotopically heavy Zn-Pb mineralization. Perhaps isotopically light framboidal pyrite formed at the chemocline at the top of a euxinic water body from microbially reduced seawater sulfate, above a dense metalliferous brine pool where Zn-Pb sulfides were precipitating. Isotopically light pyrite framboids then settled into the brine pool, and were deposited onto the seafloor with isotopically heavy sphalerite, galena and pyrite. However, pyrite growth textures, trace element-rich py2a-b in the ACTM and highly contrasting S isotope ratios between coexisting sulfides in the ACTM suggest that a diagenetic origin of Zn-Pb mineralization cannot be ruled out. Additional SIMS work is planned and will focus on better constraining the S isotope composition of framboidal pyrite from the major Zn-Pb SEDEX deposits (i.e., XYC, Don and Anniv) to gain a clearer understanding on the source(s) of S and, whether the isotopically light sulphides are widespread and an important component of mineralization along the Zinc Corridor.

Select References

Claypool, C. E., Hosler, W. T., Saki, J. R., and Zak, I., 1980, The age curves for sulfur and oxygen isotopes in marine sulfate and their mutual interpretation: Chemical Geology, v. 28, p. 199-260.
Goodfellow, W.D. (2004): Geology, genesis and exploration of SEDEX deposits, with emphasis on the Selwyn Basin, Canada, in Deb, M., and Goodfellow, W.D., eds., Sediment-Hosted Lead-Zinc Sulphide Deposits: Attributes and Models of Some Major Deposits of India, Australia and Canada: Narosa Publishing House, Delhi, India, p. 24-99.
Goodfellow, W. D., and Jonasson, I. R., 1984, Ocean stagnation and ventilation defined by $\delta^{34}S$ values in pyrite and barite, Selwyn Basin, Yukon: Geology, v. 12, p. 583-586.
Goodfellow, W. D., and Jonasson, I. R., 1986, Environment of formation of the Howards Pass (XY) Zn-Pb deposit, Selwyn Basin, Yukon, in Morin, J. A., ed., Mineral Deposits of Northern Cordillera, 37. Special Volume, Canadian Institute of Mining and Metallurgy, p. 19-50.
Jonasson, I.R. and Goodfellow, W.D. (1986): Sedimentary and diagenetic textures, and deformation structures within sulphide zone of Howards Pass (XY) Zn-Pb deposit, Yukon and Northwest Territories, in Morin, J.A., ed., Mineral Deposits of the Northern Cordillera: Canadian Institute of Mining and Metallurgy, Special Volume 37, p. 51-70.
Gordey, S.P. and Anderson, R.G. (1993): Evolution of the Northern Cordilleran Miogeocline, Nahanni Map Area (105I), Yukon and Northwest Territories. Geological Survey of Canada Memoir 428, 214 p.
Sweeney, R. E., and Kaplan, I. R., 1980, Stable isotope composition of dissolved sulfate and hydrogen sulfide in the Black Sea: Marine Chemistry, v. 9, p. 145-152.